

Thermodynamic and Structural Properties analysis of Li_3OI Using Density Functional Theory

¹Iram Shahzadi, ²Ghazia Bashir, ^{3,*}Javaria Batool

^{1,2,3} Govt College Women University, Faisalabad, Punjab, Pakistan; * Govt. Islamia Graduate College for Women, Eidgah road Faisalabad

Email: iiram9237@gmail.com, ghaziabashir447@gmail.com, javariabatoolpk@gmail.com*

ABSTRACT

First principle based, full potential linearized augmented plane-wave plus local-orbitals (FPLAPW+LO) density functional theory calculations are used to examine the thermodynamic and structural properties of Li_3OI . The phase diagram of Li_3OI is calculated via thermodynamic potentials that offered crucial information about stable synthesis of material. The obtained restriction of chemical atomic potential values of Li, I and O provides information about stable synthesis of Li_3OI . Our calculated results clarify the background of experimentally for the synthesis of Li_3OI and related binary phases.

Keywords: Antiperovskite material; Density functional theory, Phase diagram, structural properties; Enthalpy of formation;

1 INTRODUCTION:

Owing the part of solid state electrolyte for lithium ion batteries attained great achievements in customer electronics. Due to growing demand of energy storage devices alkali metal based antiperovskite plays an important role in electrolytes [30]. We found promising application of solid electrolytes which has made these materials relevant for use in electrical vehicles, batteries, mobile phones, digital cameras, stationary and portable [34], [33]. Now a day's batteries are the important part of our life. We cannot even imagine living life without batteries concept. Lithium ion batteries [3] boast high energy density. Lithium ions have a longer run time between the charging [23]. Lithium based batteries are last longer and have greater energy than of sodium ion batteries [32], [13]. It has the lot of potential material used of cathode, the part of the battery that receives the flowing electrons. Lithium ions are dominated in the market due to phones, laptops, electric cars and many electronic devices [12]. Due to significant applications and use of Lithium Oxide Iodide (LOI) antiperovskite material we research on Li_3OI anti perovskites material by using Generalized Gradient Approximation method (GGA) [26]. Antiperovskite accumulates are of much logical interest in light of their easygoing actual properties, for example, giant magneto resistance almost zero temperature coefficient of opposition. Contingent upon the compound creation, these materials can show a variety of properties like semiconducting, attractive, and super directing properties. For instance, Lithium based antiperovskite Li_3OI , Li_3OBr , Li_3OCl [27] show semiconducting properties [9], [8]. Taking into account these significant uses of antiperovskite it is beneficial to think about their actual properties more exhaustively. Among the known antiperovskite compounds, the salt metal halide compounds are somewhat neglected for their physical and synthetic properties [10]. Since the constructions of these mixtures contain strange mixes of compound components it would be very fascinating to know their fundamental physical and synthetic properties [2]. Albeit these materials have superb electronic

[18] and holding properties just a couple of studies are accessible on these mixtures in writing. Supposedly there are no investigations from the test or hypothetical side on the electronic, holding, flexible, and optical properties of these mixtures [21]. The information on electronic band design and thickness of states is needed to comprehend the leading nature and the kind of holding present in the materials as far as the band hole and the hybridization of various nuclear states in the materials [4],[14]. They are likewise helpful in understanding the different optical changes that are conceivable. The optical properties, like the assimilation range and the dielectric work, can be utilized to decide the optical band hole and dielectric constants, which are of principal significance in displaying the semiconducting gadgets. In this paper, we present a progression of first-standards computations on the primary, electronic, structural, thermodynamics and optical properties of antiperovskite Lithium Oxide Iodide (LOI) Li_3OI . The versatile constants and along these lines distinctive flexible moduli are determined which are additionally used to examine the structural properties conduct of the metal halides [20]. The optical properties, for example, the dielectric work, reflectivity, retention, refractive list, and electron energy-misfortune work are determined and examined [22]. We studied electronic, structural, optical and thermodynamic properties of LOI in this paper.

Additionally, there could be no prior estimations about the strain impact on the electronic and optical properties of these mixtures have been finished. On the opposite side, till now no hypothetical investigation utilizing a maximum capacity technique has been performed on these materials (“V.I. Gavrilov,” 1975). The reasons referenced above inspire us to play out these computations, utilizing the best in class maximum capacity increased plane wave plus local orbital approach (FP-APW+lo) in light of the density functional theory (DFT)[17], [11].

The remaining paper has been divided into three parts. In section 2 we briefly describe the computational techniques used in the study. The most relevant results obtained for the structural and thermodynamic properties of Li_3OI . Lastly summarize the whole work.

2 COMPUTATIONAL DETAILS

We use WIEN2K code which utilized Full-potential linear-augmented plan wave (FP+LAPW) [24] of density functional theory (DFT) for computing the electronic properties of Li_3OI for the exchange correlation functional of lithium oxide iodide LOI. We use Perdew- Burke- Ernzerhof generalized gradient approximation (PBE-GGA) parameters. By using GGA method we firstly calculate the structural properties of Li_3OI . We found ground state energy and lattice constant of LOI, which is $a=b=c= 4.26$ which is approximately equal to experimental value of lattice constant of LOI (F. Wang et al., 2020) [12]. The ground state energy of LOI is $-14434.18997056\text{Aug}$. Where the energy of Li, O, I, Li_2O , LiI are given in table no 2.1.

We use GGA method for the calculation of optical, structural, electronic, and thermodynamic properties of Li_3OI . We also find distance between two elements which is called bond length (Dawson et al., 2018). The bond length of Li-I is 2.9426Aug , I-I is 4.1614Aug , I-O is 3.6039Aug , Li-Li is ___ and Li-O is also. The Li_3OI antiperovskite material has a cubic structure with $\text{pm}3\text{m}$ crystallography (221) space group [25]. To study the effect of DFT methods on the formation energy [7] E_f of Li_3OI we compare the results using GGA functional [19], [34] At the end of testing the optimal K- point grid and the energy cutoff, an energy cutoff ___ eV and a k- point grid of $5 \times 5 \times 5$ were selected for the energy optimization and calculation [1], [15]. The lattice parameters are obtained by using different method and the experimental results are available in table.

Table 1

Compounds ground state energy with lattice constant

No. of compound	Compound name	Ground state energy (Ry)	Lattice constant (Å)
1	Li	-15.03911485	2.7255
2	O	-150.3396187	0.5000
3	I	-56952.45842284	4.7348
4	Li ₂ O	-180.86531437	4.6292
5	LiI	-14253.31376703	3.7873
6	Li ₃ OI	-14434.18997056	4.612

3. Result and Discussion

We computed the ground state energy for structural properties and also calculate enthalpy of formation with the help of GGA method. Further the thermodynamics properties [6] of binary compounds of LOI also calculated that play an important role in restricting the chemical potential limits of Li, I and O for stable synthesis of LOI.

3.1 Structural Properties of Li₃OI

To evaluate the structural properties [31] of LOI antiperovskite compound by using GGA method from volume optimization. We found LOI have cubic crystal structure with experimental value 4.61Å. The experimental data is given in table.

Table 2

Show the theoretical structural properties of LOI including space group (S_g), lattice parameters (L_p), band gap (B_{gap}) bond angle (B_{angle}) and tolerance factor (T_f)

Compound	S_g	L_p (Exp.)	L_p (Throe.)	B_{gap}	B_{angle}	T_f
Li ₃ OI	221 (Pm $\bar{3}$ m)	4.162Å	4.1612Å	3.927Ev	90°	0.98 ^a

In table 3.1 shows the computed structural parameters of LOI along with prior experimental study. Comparison of lattice parameters data with experimental values clearly indication that the standard overestimation of the lattice parameters with GGA. In all cases our calculated theoretical value of lattice parameter is 0.99% less than from experimental value.

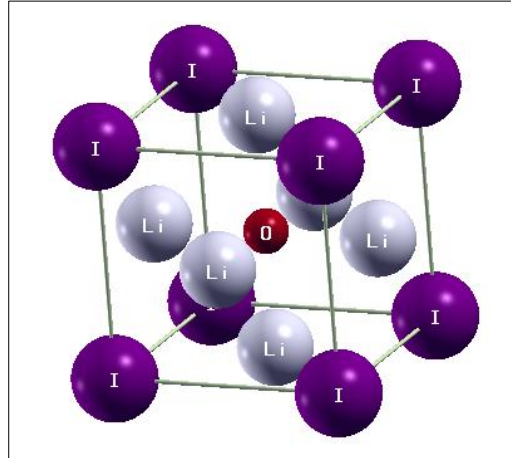


Figure 3. 1 Crystal structure diagram of Li₃OI by using GG approximation

3.2 Phase diagram of Li₃OI

To estimate the thermodynamic properties of LOI compound by DFT calculation is an appropriate method. For this purpose it is essential to compute ground state energies from structural properties (SP) of LOI. We corresponding total energy of material from SP and its competing binary phase. The simplest chemical reaction finding from LOI with the two binary compounds is LiI and Li₂O.

Phase diagram represent the legal series of atomic chemical potentials of LOI. We assume chemical potential of atoms in their stable state with valid range of ground state energy obtain from volume optimization. We obtain phase diagram from the values of chemical potential of LOI. We use general formula as shown in equation (1) for the calculation of chemical potential.

$$\mu_A = \mu_A^{gas/solid} + \Delta\mu \quad (1)$$

From the above assumption the values of the atomic potential or chemical potential (Batool et al., 2017) of Li, O and I requisite satisfy such as

$$\Delta\mu_{Li} + \Delta\mu_I \leq \Delta H_f^{LiI} \quad (2)$$

$$2\Delta\mu_{Li} + \Delta\mu_O \leq \Delta H_f^{Li_2O} \quad (3)$$

$$3\Delta\mu_{Li} + \Delta\mu_I + \Delta\mu_O = \Delta H_f^{Li_3OI} \quad (4)$$

The values of enthalpy of formation of LOI, Li₂O and LiI can be easily calculated by using below equation.

$$\Delta H_f^{Li_3OI} = E_t^{Li_3OI} - 3E_t^{Li} - E_t^I - \frac{1}{2}E_t^{O_2} \quad (5)$$

$$\Delta H_f^{Li_2O} = E_t^{Li_2I} - 2E_t^{Li} - \frac{1}{2}E_t^{O_2} \quad (6)$$

$$\Delta H_f^{LiI} = E_t^{LiI} - E_t^{Li} - E_t^I \quad (7)$$

Wherever $E_t^{Li_3OI}$, $E_t^{Li_2O}$, E_t^{LiI} , E_t^{Li} and E_t^I are the minimum total energy of GGA optimized cell of Li_3OI , Li_2O , LiI , Li , I respectively. It is obvious from table 3.2 that the computed enthalpies of formation come to an understanding well with offered experimental data.

Table 3

Comparison of experimental enthalpy of formation values of LiI, Li₂O and Li₃OI with theoretical data

Compound	Enthalpies of formation (eV f. u ⁻¹)	
	Calculated	Experimental
ΔH_f^{LiI} (space group # 225, Fm $\bar{3}$ m)	- 2.1775439 47	-2.737 ^b
$\Delta H_f^{Li_2O}$ (space group # 229, Fm $\bar{3}$ m)	- 6.0880867 47	-6.1415 ^a
$\Delta H_f^{Li_3OI}$ (space group # 221, Pm $\bar{3}$ m)	- 8.4137853 17	—

.a Ref (Kimura, Hitoshi and Asano, Mitsuru and Kubo, Kenji) (Kimura, Hitoshi and Asano, Mitsuru and Kubo, Kenji, 1980) b Ref (Nasar, Abu, 2013)

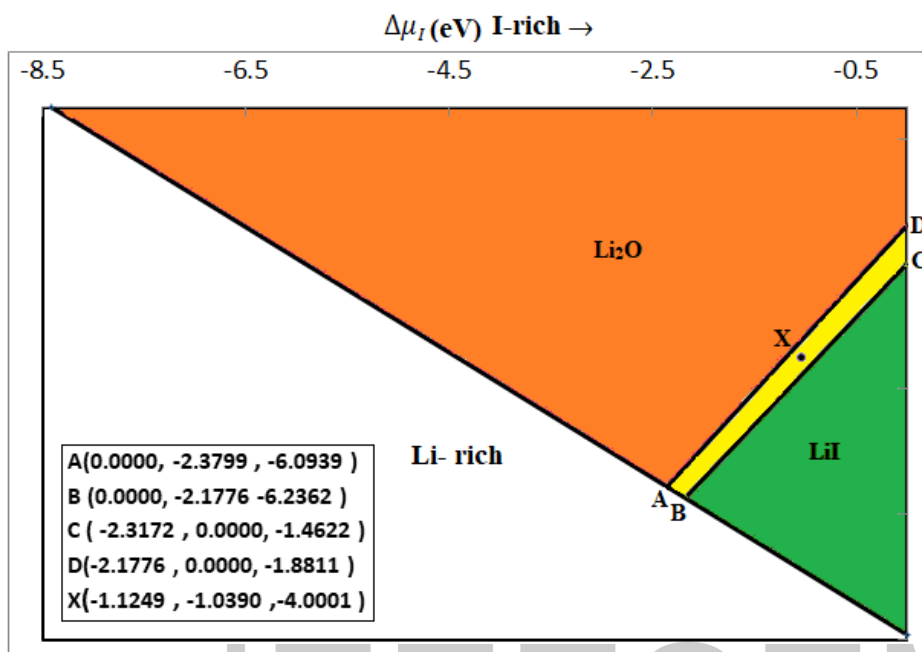


Figure 3.2 phase diagram of Li_3OI , in which A, B, C and D fenced in the region within Li_3OI can be synthesized without the presence of binary phase of Li_2O and LiI .

The sum of enthalpy of formation of Li_2O and LiI is less than the enthalpy of formation of LOI . With the help of enthalpy of formation (Emly et al., 2013) we computed phase diagram of LOI as shown in figure 3.2. in the phase diagram the area enclosed by the points A-B-C-D signify thermo dynamical stability of LOI without formation of binary phase of Li_2O and LiI .

The points A and B are shown in figure gives the Li-rich states where C and D points satisfy the I-rich state. The Li-poor and I-poor states are fulfilled at point D and A point respectively. While over the O-rich and O-poor states are fulfilled at point D and B. the stable points of phase diagram offered us the valid ranges of atomic potential ($(\Delta\mu_{\text{Li}}, \Delta\mu_{\text{I}}, \Delta\mu_{\text{O}})$) that show the intrinsic vacancy in terms of formation energy in LOI .

4 Conclusion

Density function theory calculations have been done with the evolution of thermodynamic stability and structural properties of pristine and intrinsic vacancy defect containing LOI . Our computed phase diagram of LOI express good agreements with experimental values and offer precise limits of atomic potential of Li, I and O. We initiate that our results depend upon the chemical environment that allow alteration these properties of LOI during experimental synthesis.

Reference

1. Ahiavi, E., Dawson, J. A., Kudu, U., Courty, M., Islam, M. S., Clemens, O., Masquelier, C., & Famprikis, T. (2020). Mechanochemical synthesis and ion transport properties of Na₃OX (X = Cl, Br, I and BH₄) antiperovskite solid electrolytes. *Journal of Power Sources*, 471, 228489. <https://doi.org/10.1016/j.jpowsour.2020.228489>
2. Amara, K., Zemouli, M., Elkeurti, M., Belfedal, A., & Saadaoui, F. (2013). First-principles study of XNMg₃ (X=P, As, Sb and Bi) antiperovskite compounds. *Journal of Alloys and Compounds*, 576, 398–403. <https://doi.org/10.1016/j.jallcom.2013.06.003>
3. Arshad, F., Li, L., Amin, K., Fan, E., Manurkar, N., Ahmad, A., Yang, J., Wu, F., & Chen, R. (2020). A Comprehensive Review of the Advancement in Recycling the Anode and Electrolyte from Spent Lithium Ion Batteries. *ACS Sustainable Chemistry & Engineering*, 8(36), 13527–13554. <https://doi.org/10.1021/acssuschemeng.0c04940>
4. Azouaoui, A., Benzakour, N., Hourmatallah, A., & Bouslykhane, K. (2021). Investigation of structural, electronic, magnetic, elastic and thermodynamic properties of Mn₃GaN antiperovskite by first principle and Monte Carlo simulations. *Philosophical Magazine*, 101(13), 1587–1601. <https://doi.org/10.1080/14786435.2021.1917782>
5. Baktash, A., Demir, B., Yuan, Q., & Searles, D. J. (2021). Effect of defects and defect distribution on Li-diffusion and elastic properties of anti-perovskite Li₃OCl solid electrolyte. *Energy Storage Materials*, 41, 614–622. <https://doi.org/10.1016/j.ensm.2021.06.039>
6. Batool, J., Alay-e-Abbas, S. M., Ali, A., Mahmood, K., Akhtar, S., & Amin, N. (2017). The role of intrinsic vacancy defects in the electronic and magnetic properties of Sr₃SnO: A first-principles study. *RSC Advances*, 7(12), 6880–6888. <https://doi.org/10.1039/C6RA25339C>
7. Batool, J., Alay-e-Abbas, S. M., & Amin, N. (2018). Thermodynamic, electronic, and magnetic properties of intrinsic vacancy defects in antiperovskite Ca₃SnO. *Journal of Applied Physics*, 123(16), 161516. <https://doi.org/10.1063/1.4994998>
8. Bidai, K., Ameri, M., Amel, S., Ameri, I., Al-Douri, Y., Varshney, D., & Voon, C. H. (2017). First-principles calculations of pressure and temperature dependence of thermodynamic properties of anti-perovskite BiNBa₃ compound. *Chinese Journal of Physics*, 55(5), 2144–2155. <https://doi.org/10.1016/j.cjph.2017.03.023>
9. Bouhemadou, A., & Khenata, R. (2007). Ab initio study of the structural, elastic, electronic and optical properties of the antiperovskite SbNMg₃. *Computational Materials Science*, 39(4), 803–807. <https://doi.org/10.1016/j.commatsci.2006.10.003>
10. Bouhemadou, A., Khenata, R., Chegaar, M., & Maabed, S. (2007). First-principles calculations of structural, elastic, electronic and optical properties of the antiperovskite AsNMg₃. *Physics Letters A*, 371(4), 337–343. <https://doi.org/10.1016/j.physleta.2007.06.030>
11. Cohen, A. J., Mori-Sánchez, P., & Yang, W. (2012). Challenges for Density Functional Theory. *Chemical Reviews*, 112(1), 289–320. <https://doi.org/10.1021/cr200107z>
12. Dawson, J. A., Attari, T. S., Chen, H., Emge, S. P., Johnston, K. E., & Islam, M. S. (2018). Elucidating lithium-ion and proton dynamics in anti-perovskite solid electrolytes. *Energy & Environmental Science*, 11(10), 2993–3002. <https://doi.org/10.1039/C8EE00779A>
13. Deng, Z., Ni, D., Chen, D., Bian, Y., Li, S., Wang, Z., & Zhao, Y. (2021). ANTI-PEROVSKITE materials for energy storage batteries. *InfoMat*, inf2.12252. <https://doi.org/10.1002/inf2.12252>
14. Durbin, R. P. (1975). Letter: Acid secretion by gastric mucous membrane. *The American Journal of Physiology*, 229(6), 1726. <https://doi.org/10.1152/ajplegacy.1975.229.6.1726>
15. Effat, M. B., Liu, J., Lu, Z., Wan, T. H., Curcio, A., & Ciucci, F. (2020). Stability, Elastic Properties, and the Li Transport Mechanism of the Protonated and Fluorinated Antiperovskite Lithium Conductors. *ACS Applied Materials & Interfaces*, 12(49), 55011–55022. <https://doi.org/10.1021/acsmi.0c17975>
16. Emly, A., Kioupakis, E., & Van der Ven, A. (2013). Phase Stability and Transport Mechanisms in Antiperovskite Li₃OCl and Li₃OBr Superionic Conductors. *Chemistry of Materials*, 25(23), 4663–4670. <https://doi.org/10.1021/cm4016222>
17. Erhart, P., & Albe, K. (2007). Thermodynamics of mono- and di-vacancies in barium titanate. *Journal of Applied Physics*, 102(8), 084111. <https://doi.org/10.1063/1.2801011>
18. Fang, H., & Jena, P. (2017a). Li-rich antiperovskite superionic conductors based on cluster ions. *Proceedings of the National Academy of Sciences*, 114(42), 11046–11051. <https://doi.org/10.1073/pnas.1704086114>
19. Fang, H., & Jena, P. (2017b). Li-rich antiperovskite superionic conductors based on cluster ions. *Proceedings of the National Academy of Sciences*, 114(42), 11046–11051. <https://doi.org/10.1073/pnas.1704086114>
20. Gardos, G., & Cole, J. O. (1976). Maintenance antipsychotic therapy: Is the cure worse than the disease? *The American Journal of Psychiatry*, 133(1), 32–36. <https://doi.org/10.1176/ajp.133.1.32>
21. Hichour, M., Khenata, R., Rached, D., Hachemaoui, M., Bouhemadou, A., Reshak, Ali. H., & Semari, F. (2010). FP-APW+lo study of the elastic, electronic and optical properties for the cubic antiperovskite ANSr₃ (A=As, Sb and Bi) under pressure effect. *Physica B: Condensed Matter*, 405(7), 1894–1900. <https://doi.org/10.1016/j.physb.2010.01.069>

22. Kidder, G. W., & Montgomery, C. W. (1975). Oxygenation of frog gastric mucosa in vitro. *The American Journal of Physiology*, 229(6), 1510–1513. <https://doi.org/10.1152/ajplegacy.1975.229.6.1510> Kimura, Hitoshi and Asano, Mitsuru and Kubo, Kenji. (1980). Thermochemical study of the vaporization of Li₂O (c) by mass spectrometric Knudsen effusion method. *Journal of Nuclear Materials*, 92, 221--228.
23. Kim, K., & Siegel, D. J. (2019). Correlating lattice distortions, ion migration barriers, and stability in solid electrolytes. *Journal of Materials Chemistry A*, 7(7), 3216–3227. <https://doi.org/10.1039/C8TA10989C>
24. Laskowski, R., & Blaha, P. (2014). Calculating NMR chemical shifts using the augmented plane-wave method. *Physical Review B*, 89(1), 014402. <https://doi.org/10.1103/PhysRevB.89.014402>
25. Morscher, A., Dyer, M. S., Duff, B. B., Han, G., Gamon, J., Daniels, L. M., Dang, Y., Surta, T. W., Robertson, C. M., Blanc, F., Claridge, J. B., & Rosseinsky, M. J. (2021). Li₆SiO₄Cl₂: A Hexagonal Argyrodite Based on Antiperovskite Layer Stacking. *Chemistry of Materials*, 33(6), 2206–2217. <https://doi.org/10.1021/acs.chemmater.1c00157>
26. Nasar, Abu. (2013). Correlation between standard enthalpy of formation, structural parameters and ionicity for alkali halides. *Journal of the Serbian Chemical Society*, 78, 241--253.
27. Ramanna, J., Yedukondalu, N., Ramesh Babu, K., & Vaitheeswaran, G. (2013). Ab initio study of electronic structure, elastic and optical properties of anti-perovskite type alkali metal oxyhalides. *Solid State Sciences*, 20, 120–126. <https://doi.org/10.1016/j.solidstatesciences.2013.03.014>
28. Reckeweg, O., Blaschkowski, B., & Schleid, T. (2012). Li₅OCl₃ and Li₃OCl: Two Remarkably Different Lithium Oxide Chlorides. *Zeitschrift Für Anorganische Und Allgemeine Chemie*, 638(12–13), 2081–2086. <https://doi.org/10.1002/zaac.201200143>
29. V.I. Gavrilov. (1975). *Acta Virologica*, 19(6), 510.
30. Wang, F., Evans, H. A., Kim, K., Yin, L., Li, Y., Tsai, P.-C., Liu, J., Lapidus, S. H., Brown, C. M., Siegel, D. J., & Chiang, Y.-M. (2020). Dynamics of Hydroxyl Anions Promotes Lithium Ion Conduction in Antiperovskite Li₂OHCl. *Chemistry of Materials*, 32(19), 8481–8491. <https://doi.org/10.1021/acs.chemmater.0c02602>
31. Wang, Y., Zhang, H., Zhu, J., Lü, X., Li, S., Zou, R., & Zhao, Y. (2020). Antiperovskites with Exceptional Functionalities. *Advanced Materials*, 32(7), 1905007. <https://doi.org/10.1002/adma.201905007>
32. Wang, Z., Xu, H., Xuan, M., & Shao, G. (2017a). From anti-perovskite to double anti-perovskite: Lattice chemistry basis for super-fast transportation of Li⁺ ions in cubic solid lithium halogen-chalcogenides. *ArXiv:1707.05868 [Cond-Mat, Physics:Physics]*. <http://arxiv.org/abs/1707.05868>
33. Wang, Z., Xu, H., Xuan, M., & Shao, G. (2017b). From anti-perovskite to double anti-perovskite: Lattice chemistry basis for super-fast transportation of Li⁺ ions in cubic solid lithium halogen-chalcogenides. *ArXiv:1707.05868 [Cond-Mat, Physics:Physics]*. <http://arxiv.org/abs/1707.05868>
34. Wang, Z., Xu, H., Xuan, M., & Shao, G. (2018). From anti-perovskite to double anti-perovskite: Tuning lattice chemistry to achieve super-fast Li⁺ transport in cubic solid lithium halogen-chalcogenides. *Journal of Materials Chemistry A*, 6(1), 73–83. <https://doi.org/10.1039/C7TA08698A>
35. Xu, H., Xuan, M., Xiao, W., Shen, Y., Li, Z., Wang, Z., Hu, J., & Shao, G. (2019). Lithium Ion Conductivity in Double Antiperovskite Li_{6.5}OS_{1.5}I_{1.5}: Alloying and Boundary Effects. *ACS Applied Energy Materials*, 2(9), 6288–6294. <https://doi.org/10.1021/acsaem.9b00861>
36. Zhao, S., Chen, C., Li, H., & Zhang, W. (2021). Theoretical insights into the diffusion mechanism of alkali ions in Ruddlesden–Popper antiperovskites. *New Journal of Chemistry*, 45(9), 4219–4226.